Article

AMERICAN SCIENTIFIC PUBLISHERS
Copyright © 2016 American Scientific Publishers
All rights reserved
Printed in the United States of America

Journal of
Nanoscience and Nanotechnology
Vol. 16, 11613–11618, 2016
www.aspbs.com/jnn

Polymer-Metal Composite Thin Film Microcap Packaging Technology Using Low Temperature SU-8 Bonding

Jinnil Choi[1], Yong-Kook Kim[2], Soo-Won Kim[2], Byung Hyun Nam[1], and Byeong-Kwon Ju[3,*]

[1] *Department of Mechanical Engineering, Hanbat National University, Daejeon 305-719, Republic of Korea*
[2] *Department of Electronics and Computer Engineering, Korea University, Seoul 136-713, Republic of Korea*
[3] *Display and Nanosystem Laboratory, College of Engineering, Korea University, Seoul 136-713, Republic of Korea*

This paper reports a packaging technology involving a lightweight, low temperature bonding process with a polymer-metal composite thin film microcap. A layer of SU-8, in the form of sealing rims, is used as an adhesive to bond the micro and nano-electromechanical systems (MEMS/NEMS) substrate with the microcap due to the excellent properties of SU-8 as a packaging material. A silicon oxide thin film layer is formed on the carrier wafer by using a furnace to separate the microcap from the carrier wafer once the bonding process between the host and the carrier wafer is complete. In addition, the thin-film polymer microcap retains its original shape and acts as a protective layer for the cavity after the carrier wafer is released. To characterize the bonding strength, tensile tests have been carried out, and the measurement results show that the bond strength is up to ~15 MPa. This means that the proposed packaging method, with the thin-film polymer microcap on the host wafer, was successfully realized by the low temperature bonding and transfer process. Finally, to check and verify the mechanical conditions, such as stress and deflection, of the microcap in the atmosphere, finite element (FE) analysis has been performed.

Keywords: Microcap Packaging, Micro/Nano-Electromechanical Systems (MEMS/NEMS), Bonding, Finite Element Analysis.

1. INTRODUCTION

For the integration of micro and nanoscale structures to produce cheaper and better quality components, micro and nano-electromechanical systems (MEMS/NEMS) technology has been applied to various devices such as switches, resonators, sensors and capacitors. Therefore, the necessity for efficient packaging of these MEMS/NEMS-based components has rapidly increased. However, it is significantly more expensive, larger and heavier than that of integrated circuit packaging and often amounts to more than 70% of the total cost of a microsystem.[1–3] The main advantages of MEMS/NEMS packaging partly involves a reduction in size and weight that it affords, but primarily lies on the potential of wafer-level packaging technology to improve the electrical performance at a comparable or even reduced manufacturing cost.

Any bonding technique must provide a relatively strong bond at the lowest possible temperature, because higher temperatures could harm the metallization layers and introduce considerable stress to the bonded materials. Adhesive wafer bonding, which is IC compatible, is superior to other established bonding techniques, such as anodic or direct bonding in terms of the process temperature. Among the various amorphous polymers, polyimides,[4,5] benzocyclobutene (BCB),[6–8] parylene,[9–11] epoxy[12] and photoresists[13] have been investigated as possible intermediate layers for wafer bonding. One of these polymers, the negative photoresist SU-8,[14–19] was used in this paper because it is a highly crosslinked epoxy-type photo-patternable polymer, and it has useful properties, including photosensitivity, transparency to visible light and high chemical and thermal stabilities as well as good mechanical characteristics. These properties have led to SU-8 being used in MEMS/NEMS fabrication to obtain movable and rigid micro and nanomechanical structures such as micro-channels, optical waveguides, wafer bonding layers, and packaging coating layers.

This paper proposes a MEMS/NEMS packaging scheme, with a low temperature bonding process, using the patternable negative photoresist SU-8. The SU-8 serves as

*Author to whom correspondence should be addressed.

 1533-4880/2016/16/11613/006 doi:10.1166/jnn.2016.13561

the microcap structure material and the bonding adhesive layer between the microcap and the host wafer. Experiments have been conducted to examine polymer bonding with the SU-8 microcap and sealing rim at a temperature of 120 °C, in which a pressure of 0.15 MPa was applied for 30 min. The SU-8 microcap was fabricated and separated, from the carrier wafer to the host wafer, using transfer technology. In comparison to general packaging methods, requiring relatively high temperature bonding, such as eutectic, anodic and fusion bonding, this packaging method involves a low temperature process. In addition, it provides a simple, easy assembly process for MEMS/NEMS packaging by utilizing SU-8 as a microcap structure and sealing material. Finally, FE analysis has been performed to verify the mechanical conditions of the experimental results.

2. EXPERIMENTAL DETAILS

The packaging structure contains two parts as follows: the silicon host wafer with the integrated MEMS/NEMS devices and the SU-8 microcap structure shown in Figure 1.

The negative photoresist SU-8-2050 (Microchem Corporation),[20] is used as the cap structure and the intermediate adhesive bonding layer. Due to its high cross-linking density after curing, the SU-8 is mechanically strong and so can be used as a structural material. The material properties of the photo-patternable SU-8 are listed in Table I.

The advantages of the SU-8 for packaging applications are that it provides a relatively low-cost, low temperature processing method that can easily be used at the wafer level. This packaging process consists of successive wafer level bonding and releasing steps. A cavity with the desired thickness is formed for the cap structure by using KOH wet etching. The thickness of the cap structure can be readily varied by spin coating different thicknesses of the SU-8 film. Once the cap silicon wafer is completely separated by wet etching, a successful SU-8 cap structure can readily be formed.

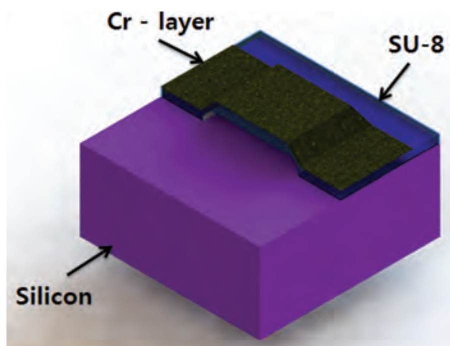

Figure 1. A schematic diagram of the proposed package structure.

Table I. Material properties of photo-patternable SU-8.

Material properties	Value
Water absorption (%85 °C/85RH)	0.65
Glass transition temperature	>200 °C
Thermal expansion linear	5.2×10^{-5}/°C
Young's modulus	4.02 GPa
Poisson's ratio	0.22
Tensile strength	60 MPa

Courtesy of F. Chollet Ed., http://memscyclopedia.org/su8.html (3 Dec. 2013).

2.1. Fabrication of the SU-8 Microcap

Figure 2 shows the fabrication process for the SU-8 microcap on the carrier wafer. A four-inch silicon wafer, with a thickness of 520 μm polished on one side is used as the carrier and host wafer. First, an oxide passivation layer was deposited on the carrier wafer and etched for use as a mask for the KOH wet etching (Fig. 2(a)). With the mask layer, the carrier wafer was anisotropically etched by 20 wt% KOH, at 80 °C, to form a cavity, until its thickness is about 70 μm (Fig. 2(b)). Then, silicon oxide (8,000 Å) was grown on the cavity surface, in a furnace (wet thermal oxidation), as a sacrificial layer for the separation process (Fig. 2(c)). The carrier wafer was cleaned in a piranha solution, at 110 °C for 10 min., and then rinsed with deionized water. Before coating with the SU-8-2050, a dehydrating treatment was performed on the wafer, at 250 °C for 30 min., to improve the adhesion of the SU-8-2050

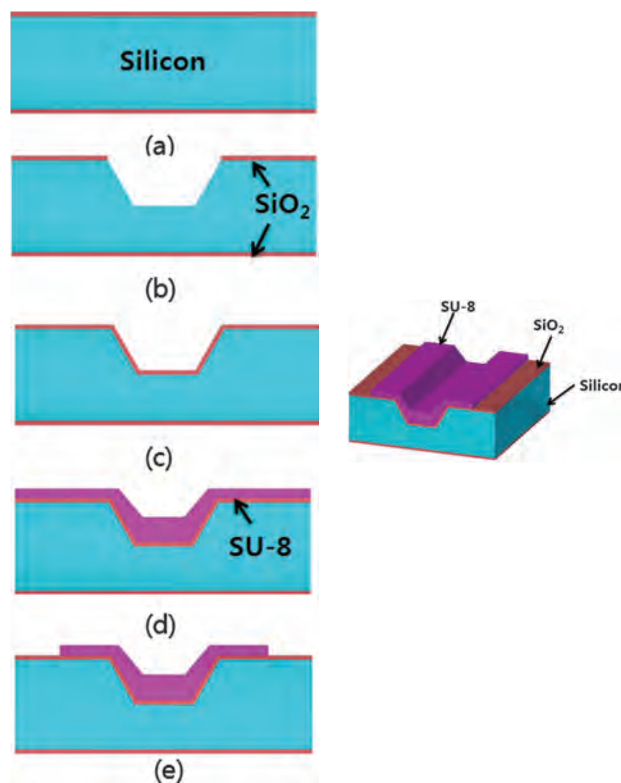

Figure 2. Cap wafer fabrication process flow. (a) Silicon wafer, (b) cavity formation, (c) thermal oxidation, (d) SU-8 coating, (e) SU-8 patterning.

film. Next, a thick photoresist (SU-8-2050) layer was spin coated with a thickness less than that of the cavity depth (70 μm) and patterned to form the bonding ring and the polymer microcap structure (Fig. 2(d)). To evaporate the solvent contained in the photo-definable materials, a soft-bake process was performed at 95 °C. Solvent-free SU-8 has low shrinkage resulting in low internal stress and better alignment registration. It also has high resistance to moisture and low weight loss.[22] Then, the post exposure bake (PEB) was performed to selectively cross-link the exposed parts of the film. The soft and post exposure bake were performed in a progressive thermal ramp to avoid photoresist microcracking. Finally, the SU-8 pattern was formed on the carrier wafer by developing it in propylene-glycol-methyl-ether-acetate (PGMEA), and rinsed in isopropanol (IPA) (Fig. 2(e)). The unexposed, and therefore not crosslinked areas, were dissolved during the development process.

2.2. Bonding Process

Before the adhesive bonding process, a 25 μm thick layer of SU-8-2050 was spin coated and patterned on a 4-inch host silicon wafer by photolithography. The line width of the bonding ring was 150 μm. The SU-8 patterned carrier wafer and the host wafer were then aligned using an optical vision system. The aligned wafer pair was then placed in the bonder (TPS-1000A, BNP Science, Korea), and the bonder chamber was evacuated to 10^{-3} mbar. The sandwich structure was pressed together in the bonder with temperature and pressure control. For bonding with the intermediate layer, the calculated contact pressure of 0.15 MPa was applied to the bonding pairs. For the curing process, the temperature was ramped linearly, from room temperature to the optimized temperature, at a rate of 3 °C min^{-1}, and the overall process time was 30 min., to fully crosslink both of the SU-8 films shown in Figure 3(a). After bonding, the bonded wafer pair was slowly cooled to room temperature, to reduce any adhesion problems caused by the different thermal expansion rates of the wafer and the SU-8 film; the influence of this bonding temperature variation on the quality of the bond was investigated.

2.3. Release Process

The next procedure is to separate the carrier wafer from the host silicon wafer. The carrier wafer can be easily separated by removing the SiO_2 layer shown in Figure 3(b). Buffered HF was used to etch the sacrificial layer between the wafers because it does not attack the SU-8. The last step provides a hermetically sealed package consisting of the polymer structure over-deposited with a metal (Cr) layer (Fig. 3(c)) in order to prevent leakage.

2.4. Numerical Analysis

In order to examine the mechanical characteristics, such as stress and deflection, numerical analysis was performed

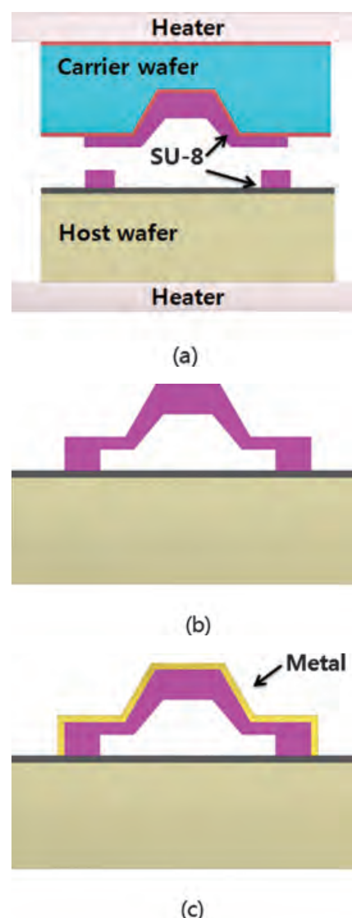

Figure 3. Polymer-metal composite microcap packaging process flow. (a) wafer level bonding process, (b) microcap separated from carrier wafer, (c) metal evaporation.

using finite element method. Mesh characteristics were defined to produce sufficient accuracy by mesh convergence analysis. Figure 4 shows the mesh generation of the numerical analysis model which consisted of various

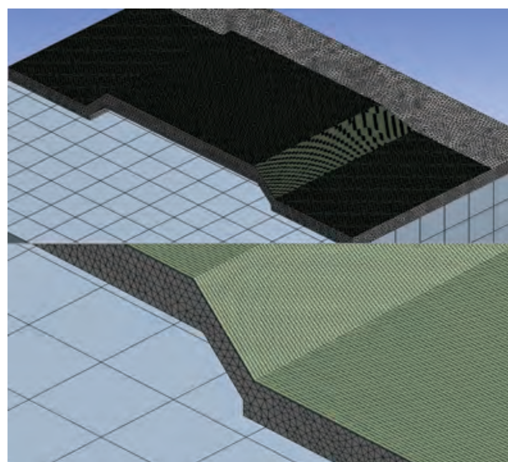

Figure 4. Contours of generated mesh for the numerical analysis model.

shapes and sizes of meshes to ensure the efficiency and accuracy of the results.

3. RESULTS AND DISCUSSION

Figure 5 shows a cross-sectional view of the bonding interface before the separation process. The sandwich structure consists of the host wafer, the SU-8 films, and the carrier wafer in the cross-section profile after the bonding process. The SU-8 films are used as an intermediate layer and microcap package structure. In this case, the bonding process was performed at a temperature of 120 °C by applying pressure of 0.15 MPa for 30 min. An adhesive layer, with a thickness of less than 25 μm, can be achieved and controlled precisely by the spin-coating process. After the bonding process, the thickness of the SU-8 layer was decreased by 2 μm, but no voids were observed in either the capping layer or the bonding interface. To quantitatively determine the strength of this bond interface, the sandwich structure was subjected to a tensile test. The measured bonding strength is high enough to allow the dicing of the wafer without the detachment or partial release of any parts of the structure. The height of the cavity, as seen in Figure 5, was determined by the thickness of the bonding rim and the SU-8 cap structure.

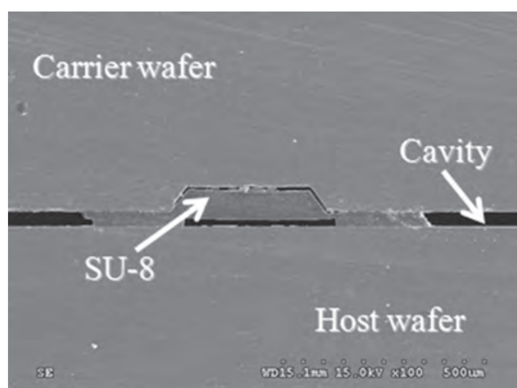

Figure 5. Cross-sectional SEM image of the bonding interface before separation process.

The SU-8 cap structure was released by etching the thermal oxide layer in buffered HF acid for 4 hours. The microcap cavity has a trapezoid shape resulting from the anisotropic bulk silicon etching. The size of the cavity in this sample is $0.8 \times 0.5 \times 0.03$ mm^3. After releasing it, the SU-8 structure is rinsed carefully in DI-water.

The bonding strength of the bonded pair, for various bonding temperatures, was measured by pull testing. For the pull test, the bonded wafers were diced using a dicing saw, and each sample was glued to a test holder using a two component epoxy glue (RP-598-2, Ablestik Co.). The pull tests were performed using the tensile tester 8848 (Instron Corporation, Canton, MA). The tensile strength measurements were carried out with 10 samples, prepared using different bonding temperatures. All of the values were averaged, and the results show average values of 12.8 MPa and 15.7 MPa, respectively, for the wafers bonded at temperatures of 100 °C and 120 °C. However, during the bonding process, the temperature increased to over 120 °C. Therefore, after the bonding process, the polymerization level of the top of the SU-8 structure layer increased shown in Figure 5. This phenomenon can affect

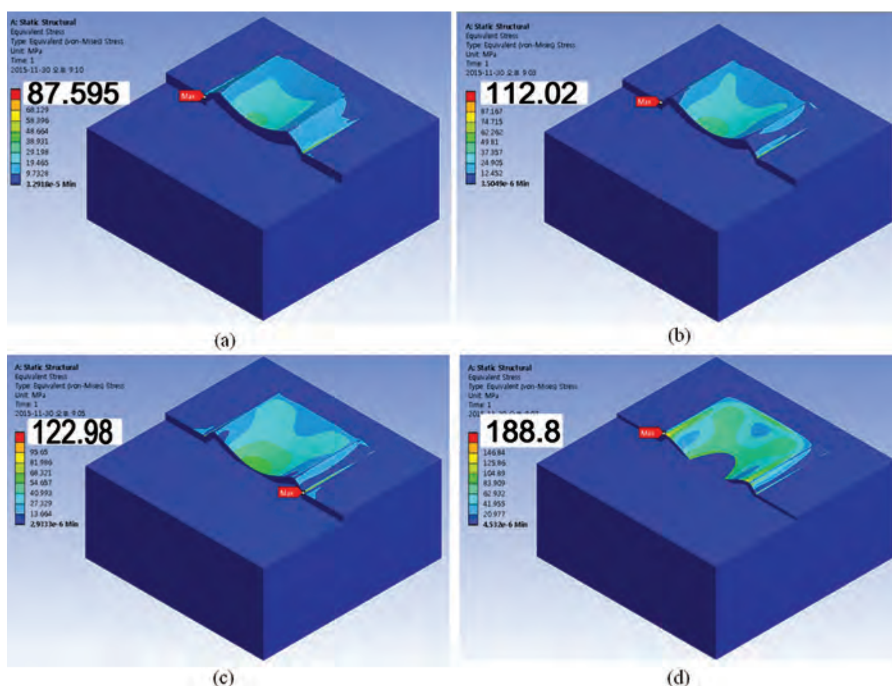

Figure 6. Contours of stress distribution for SU-8 cap structure with different SU-8 layer thickness. (a) 40 μm, (b) 30 μm, (c) 20 μm, (d) 10 μm.

Table II. Stress and deflection data for different Cr/SU-8 thickness.

Thickness [μm]	Stress [MPa]	Deflection [μm]
11	188.8	2.0435
21	122.98	0.37796
31	112.07	0.19828
41	87.595	0.11554

the mechanical stress and variation of the thickness of the SU-8 film. The non-uniformity of the SU-8 thickness causes problems in terms of the bonding quality which could lead to an increase in the non-bonded area. This problem can be minimized by decreasing the bonding temperature to around 100 °C which is sufficiently high to form a high bonding strength (12.8 MPa).

Polymers are far more permeable to gas and moisture than ceramics or metal sealants. They can be rendered hermetically, and their mechanical properties improved by the deposition of a thin metal film. However, metal Deposition can create mechanical stress in the cap layer, thus Cr films (1 μm) have been deposited on the SU-8 layer as a diffusion barrier, by using the sputtering method. To investigate the role of the Cr thin film as a protective layer for the microcap, the deformation and stress of the SU-8 layers with and without a Cr thin film were simulated and analyzed using the FEM simulation software. Prior to the investigation, examination of the mesh quality has been performed by varying the number of nodes and elements to ensure the accuracy of the developed model, for which the convergence of data was confirmed. The simulation conditions were as follows: the thickness of the Cr layer was 1 μm, and the thickness of the SU-8 microcap (370 μm $\times$ 670 μm) layer varied from 10 μm to 40 μm, and a pressure of 1 atm was applied on the top of the layer. The effects of different SU-8 thickness were investigated shown in Figure 6.

It was observed that when the thickness of the SU-8 was less than 10 μm, the Cr layer was subjected to a stress of 188.8 MPa, higher than its fracture stress (160 MPa). In order to use the Cr layer as a protective layer, a thickness of 40 μm was selected (see Table II).

Upon applying pressure to the surface of the 40 μm thick SU-8 cap layer without a Cr thin film, the maximum deflection was 0.351 μm (Fig. 7(a)); and the maximum stress (7.138 MPa) was observed at the inside edges near the top layer (Fig. 7(b)), this is because the deflection occurred near the center of the SU-8 layer. However, when applying the pressure to the surface of the Cr/SU-8 layers whose thickness was 41 μm, the maximum deflection (0.116 μm) is observed at the center of the microcap (Fig. 7(c)), and the maximum stress (87.60 MPa) appears at the outside edges near the substrate (Fig. 7(d)), due to the higher Young's modulus of the Cr layer (E = 279 GPa).[23] In this case, the maximum stress of the Cr layer is 87.60 MPa, which is lower than its fracture stress. Therefore, the Cr layer is able to protect the SU-8 layer under these conditions. Moreover, the deformation of the Cr/SU-8 layers is smaller than that of the SU-8 layer alone due to the pressure being decentralized toward the surface of the Cr layer.

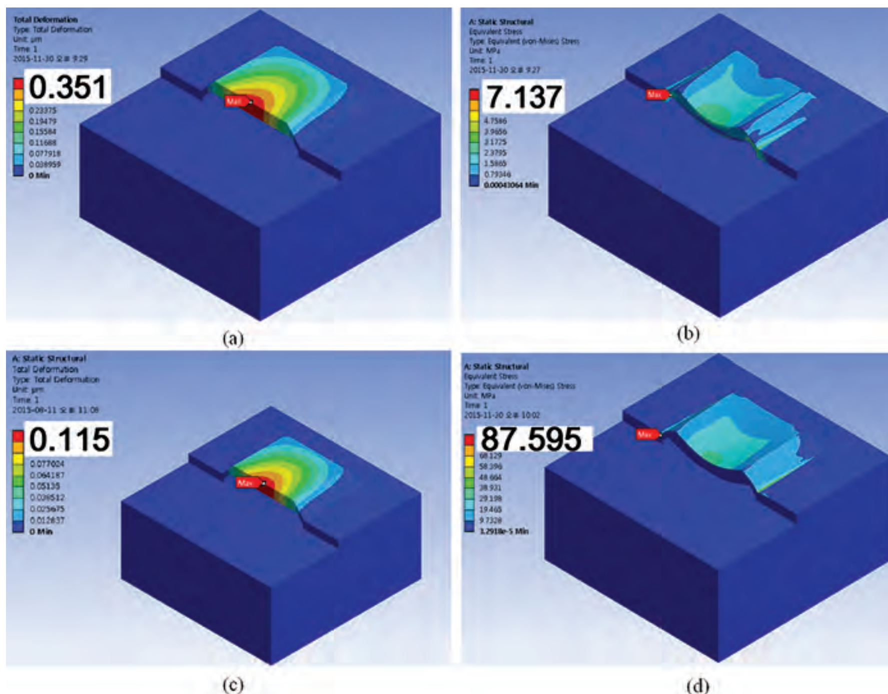

Figure 7. FE analysis of the SU-8 cap structure (thickness = 40 μm) at a pressure of 1 atm: (a) Maximum deflection, (b) stress distribution. FE analysis of a Cr/SU-8 cap structure (total thickness = 41 μm) at a pressure of 1 atm: (c) Maximum deflection, (d) Stress distribution.

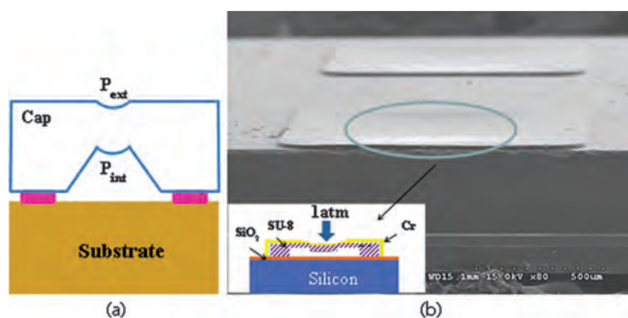

Figure 8. (a) A schematic diagram of the package with $P_{\text{ext}} > P_{\text{int}}$ and (b) SEM image of the microcap structure.

Figure 8(b) shows the completely fabricated microcap structure. No cracks were observed in the Cr/SU-8 cap structure after the whole packaging process. The SU-8 microcap was deflected towards the inside of the cavity as a result of the pressure difference, where the external pressure (P_{ext}) is larger than the internal pressure (P_{int}) shown in Figure 8(a). This confirms minimized leakage as a result of sufficient hermetic sealing of the package. After dicing, each chip contains an individual microcap, which serves to protect the MEMS/NEMS devices.

4. CONCLUSION

In this study, SU-8 microcap based packaging was proposed for MEMS/NEMS devices. The SU-8, as an adhesive bonding material, was used as the cap structure material and the SU-8 microcap was fabricated on the carrier wafer and then transferred to the host wafer using transfer technology. The SU-8 adhesive bonding showed a strong bonding strength, and the measured tensile strength of the package was in the range of 11–15 MPa. To investigate the effects of the Cr layer, a FEM model was developed, in which the use of a Cr layer as a protective layer was justified. This packaging method provides a simple, easy assembly, low cost, and low temperature process for MEMS/NEMS packaging. It is expected that the proposed low temperature adhesive bonding with SU-8 can be applied to wafer-level packaging of many MEMS/NEMS devices. In the future, further studies will be performed subjecting devices packaged with this method to thermal cycle and leak rate testing.

Acknowledgment: This research was supported by the Basic Science Research Program through the National Research Foundation of Korea (NRF) funded by the Ministry of Science, ICT and Future Planning (NRF-2014R1A1A1008010).

References and Notes

1. R. A. M. Receveur, M. Zickar, C. Marxer, V. Larik, and N. F. de Rooij, *J. Micromech. Microeng.* 16, 676 (**2006**).
2. S. A. Tadigadapa and N. Najafi, *J. Manuf. Sci. Eng.* 125, 816 (**2003**).
3. Y. Kim, H. Lee, X. Zhang, and S. Park, *IEEE. T. Compon. Pack A* 4, 1589 (**2014**).
4. R. Goggin, J. Wong, B. Hecht, P. Fitzgerald, and M. Schirmer, *J. Micromech. Microeng.* 11, 100 (**2001**).
5. M. Dhakshnamoorthy, S. Ramakrishnan, S. Vikram, N. K. Kothurkar, M. Rangarajan, and R. Vasanthakumari, *J. Nanosci. Nanotechno.* 13, 1 (**2013**).
6. J. Oberhammer, F. Niklaus, and G. Stemme, *Sens. Actuators A* 105, 297 (**2003**).
7. A. Jourdain, P. D. Moore, K. Baert, I. D. Wolf, and H. A. C. Tilmans, *J. Micromech. Microeng.* 15, 89 (**2005**).
8. M. Makihata, S. Tanaka, M. Muroyama, S. Matsuzaki, H. Yamada, T. Nakayama, U. Yamaguchi, K. Mima, Y. Nonomura, M. Fujiyoshi, and M. Esashi, *J. Micromech. Microeng.* 21, 085002 (**2011**).
9. H. Kim and K. Najafi, *J. Microelectromech. Syst.* 14, 1347 (**2005**).
10. H. S. Noh, K. S. Moon, A. Cannon, P. J. Hesketh, and C. P. Wong, *J. Micromech. Microeng.* 14, 625 (**2004**).
11. J. Charmet, J. Bitterli, O. Sereda, M. Liley, P. Renaud, and H. Keppner, *J. Microelectromech S* 22, 855 (**2013**).
12. Y. K. Kim, E. K. Kim, S. W. Kim, and B. K. Ju, *Sens. Actuators A* 143, 323 (**2008**).
13. C. T. Pan, H. Yang, S. C. Shen, M. C. Chou, and H. P. Chou, *J. Micromech. Microeng.* 12, 611 (**2002**).
14. G. Kotzar, M. Freas, P. Abel, A. Fleischman, S. Roy, C. Zorman, J. M. Moran, and J. Melzak, *Biomaterials* 23, 2737 (**2002**).
15. R. J. Jackman, T. M. Floyd, R. Ghodssi, M. A. Schmidt, and K. F. Jensen, *J. Micromech. Microeng.* 11, 263 (**2001**).
16. M. Agirregabiria, F. J. Blanco, J. Berganzo, M. T. Arroyo, A. Fullaondo, K. Mayora, and J. M. Rauanolopez, *Lab Chip* 5, 545 (**2005**).
17. S. Tuomikoski and S. Franssila, *Phys. Scr.* T114, 223 (**2004**).
18. K. N. Chen, C. A. Cheng, W. C. Huang, and C. T. Ko, *J. Nanosci. Nanotechno.* 11, 6969 (**2011**).
19. K. N. Chen, C. T. Cheng, Z. C. Hsiao, H. C. Fu, and W. C. Lo, *J. Nanosci. Nanotechno.* 12, 1821 (**2012**).
20. http://www.microchem.com/products.
21. F. Chollet, (ed.), http://memscyclopedia.org/su8.html, December (**2013**).
22. S. Tuomikoski and S. Franssila, *Sens. Actuators A* 120, 408 (**2005**).
23. H. Bourouina, R. Yahiaoui, B. Y. Majils, A. Hassein-Bey, M. E. A. Benamar, and A. Sahar, *Appl. Mech. Mater.* 8, 958 (**2014**).

Received: 1 December 2015. Accepted: 7 April 2016.